Chinese Chemical Letters 36 (2025) 110449

Contents lists available at ScienceDirect

Chinese Chemical Letters

journal homepage: www.elsevier.com/locate/cclet

A composite hydrogel with porous and homogeneous structure for efficient osmotic energy conversion

Guilong Li, Wenbo Ma, Jialing Zhou, Caiqin Wu, Chenling Yao, Huan Zeng, Jian Wang*

College of Materials and Chemistry & Chemical Engineering, Chengdu University of Technology, Chengdu 610059, China

ARTICLE INFO

Article history:
Received 24 June 2024
Revised 10 September 2024
Accepted 11 September 2024
Available online 12 September 2024

Keywords:
Osmotic energy
Cation-selective membrane
Porous structure
Stability
Power density

ABSTRACT

With the impact of energy crisis and environmental problems, it is urgent to develop green sustainable energy. Osmotic energy stored in the salinity difference between seawater and river water is one of the sustainable, abundant, and renewable energy. However, the membranes used to capture osmotic energy by reverse electrodialysis (RED) always suffer from low ion selectivity, low stability and low power. Hydrogels with three-dimensional (3D) networks have shown great potential for ion transportation and energy conversion. In this work, based on the homogeneity and porosity characteristics of acrylamide (AM) hydrogel, as well as the remarkable stability and abundant negative charge of 3-sulfopropyl acrylate potassium salt (SPAK), a high-performance AM/SPAK cation-selective hydrogel membrane was successfully developed for harvesting osmotic energy. Compared to AM hydrogels, utilizing AM/SPAK as a monomer mixture greatly facilitated the preparation of homogeneous polymers, exhibiting a porous structure, exceptional ion selectivity, and remarkable stability. A maximum output power density of 13.73 W/m^2 was achieved at a 50-fold NaCl concentration gradient, exceeding the commercial requirement of 5 W/m^2. This work broadens the idea for the construction and application of composite hydrogel in high efficiency osmotic energy conversion.

Under the threat of energy crisis, osmotic energy is considered a promising alternative to fossil fuel burning owing to its cleanliness, renewability and abundance [1,2]. Based on global river discharge to the ocean, the total hypothetical energy available from salinity gradients is in the range of 1.4–2.6 TW. At present, energy harvesting devices based on ion selective membranes can efficiently capture osmotic energy and convert it into electrical energy [3]. Reverse electrodialysis (RED) has been developed as a key technology toward harvesting osmotic energy [4]. In a RED system, the anion/cation selective membranes placed between salt solutions with different concentrations play vital roles for directly converting osmotic energy into available electric power [5-9]. However, the commonly used RED technology to obtain osmotic energy has some shortages, such as poor ion selectivity, excessive internal membrane resistance, low ion flux and poor stability, leading to low osmotic energy conversion efficiency, power density, and cannot meet commercial standards [10,11].

Inspired by biological ion channels, artificial ion channels have been extensively explored to harvest osmotic energy [12-15]. By controlling the structure and surface properties of channel membranes, the ion transport behavior can be controlled and the osmotic energy can be efficiently captured using reverse electrodialysis [14,16,17].

Hydrogel, a “soft and wet” material with a 3D network structure, shows potential in facilitating fast mass transport of ions/electrons with its interconnected pathways and the ability of being space charged [18,19]. In this work, we constructed a polyacrylamide-based anionic hydrogel with acrylamide (AM) and 3-sulfopropyl acrylate potassium salt (SPAK) as network for harvesting osmotic energy. At the same time, AM monomer hydrogel was prepared for comparison. Due to the advantages of porosity from AM and the presence of amino groups, the hydrogel can facilitate ion transport while ensuring wettability [20,21]. And SPAK is an ionic monomer with a large number of sulfonic acid groups on its surface, having a high charge density [22]. The high densities of sulfonic and amino groups make hydrogel contain a high concentration of counter ions and generate high ion selectivity [23]. Compared with AM hydrogels, the prepared composite hydrogels broke the trade-off between selectivity and permeability, improving power density with high cation selectivity. Benefiting from ultrahigh ion selectivity and porous structure, the AM/SPAK hydrogel achieved a maximum output power of 13.73 W/m^2 at a 50-fold NaCl concentration gradient. This work demonstrates that the com-

* Corresponding author.
E-mail addresses: wangjian@mail.ipc.ac.cn, wangjian17@cdut.edu.cn (J. Wang).

https://doi.org/10.1016/j.cclet.2024.110449
1001-8417/

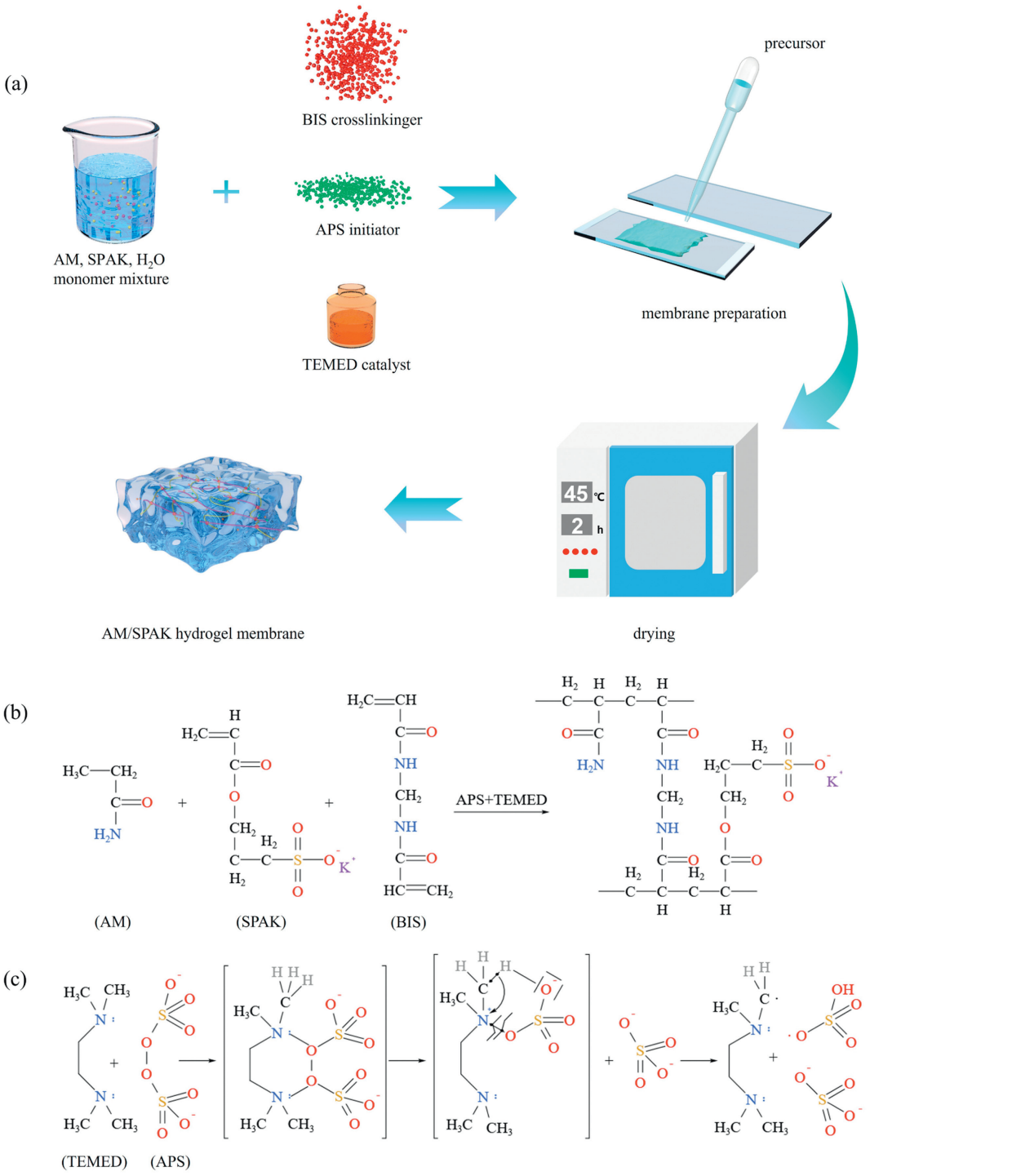

Fig. 1. (a) Schematic for preparation of the AM/SPAK hydrogel membranes. (b, c) Chemical reaction equations of the AM/SPAK hydrogel.

posite hydrogel has an excellent osmotic energy harvesting performance, broadening idea for the efficient utilization of green energy.

Fig. 1a shows the synthetic route of AM/SPAK hydrogel membrane. Firstly, different molar ratios of AM and SPAK (1:1, 2:3, 3:2) were mixed with water in the beaker, then stirred with a magnetic stirrer to achieve a homogeneous solution. After that, *N*,*N*′-methylenebisacrylamide (BIS) as a crosslinker was added into the beaker. Next, ammonium persulfate (APS) initiator and tetramethylethylenediamine (TEMED) catalyst were added to the solution as soon as possible. Subsequently, the prepared solution was dripped onto a slide (25.4 mm × 76.2 mm) with a pipette at a uniform rate, and then another slide of the same size was slowly covered on the surface of the solution. Finally, it was placed in the oven and dried for 2 h at 45 °C to obtain three-dimensional porous hydrogel membranes. Figs. 1b and c show the chemical reaction equations of the AM/SPAK hydrogel. This reaction is a vinyl addition polymerization initiated by a free radical-generating system. Polymerization is initiated by APS and TEMED, where TEMED accelerates the formation rate of free radicals from APS and thus free radicals in turn catalyze polymerization. APS radicals convert AM and SPAK monomers into free radicals, which subsequently react with inactivated monomers, initiating the polymerization chain re-

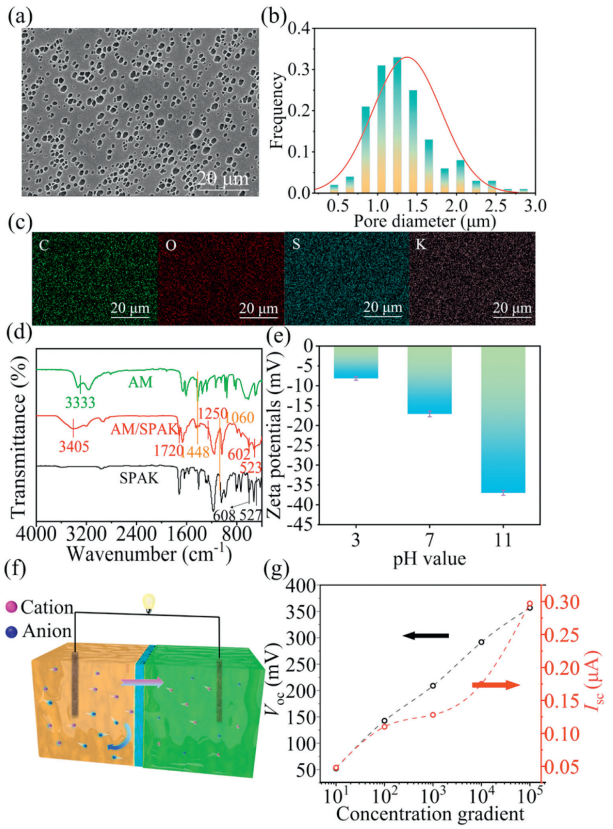

Fig. 2. Characterizations of the AM/SPAK hydrogel membrane. (a) SEM micrograph of the AM/SPAK hydrogel. (b) Pore size distribution corresponding to (a). (c) EDS mappings of the AM/SPAK hydrogel. (d) FTIR spectra of AM, AM/SPAK hydrogel membranes and SPAK. (e) Zeta potentials of the AM/SPAK hydrogel with a 1:1 molar ratio at different pH values. (f) Schematic of the experimental setup for ion transport and osmotic energy conversion of the hydrogel membrane. (g) V_{oc} and I_{sc} of the AM/SPAK hydrogel membrane as a function of the salt concentration gradient.

action. Thus, the elongated polymer chains are cross-linked by BIS to form a gel with multiple porosity [24].

Figs. 2a and b show the scanning electron microscopy (SEM) image of the AM/SPAK hydrogel surface and its corresponding pore size distribution. There are a large number of pores, with diameter between 0.8 μm and 1.5 μm, which is due to the porous and homogeneous nature of the gel formed using AM [25]. In addition, the energy dispersive X-ray spectroscopy (EDS) mapping of the hydrogel membrane was performed. Fig. 2c shows the EDS spectrum of the AM/SPAK hydrogel, with C, O, S and K elements uniformly distributed on the surface.

As shown in Fig. 2d, Fourier-transform infrared spectroscopy (FTIR) was used to investigate the chemical structure of the prepared hydrogels. Amino group at 3405 cm^{-1} ensure the wettability of the membrane surface, and amino group is a hydrophilic group, which is conducive to ion transport. Located at 523 cm^{-1} is sulfonic acid group, which can provide plentiful negative charges, thereby the polymerized hydrogel membrane has good electrical conductivity and high-power density. The C=O, C–N and C-S groups are appeared at 1720, 1250 and 602 cm^{-1}, respectively. The C=C stretching vibration peak at 1448 cm^{-1} and the O=S out-of-plane bending vibration peak at 1060 cm^{-1} on the sulfonic acid group are significantly reduced, indicating cross-linking between polymer chains [26,27]. In addition, the X-ray photoelectron spectroscopy (XPS) results show the elemental compositions of the prepared AM/SPAK hydrogel membrane (Fig. S1 in Supporting information), also indicating the successful reaction [28].

The zeta potentials of the AM/SPAK hydrogel at different pH conditions were measured with a zeta potential analyzer (ZS90). As shown in Fig. 2e and Fig. S2 (Supporting information), the zeta potentials of AM/SPAK hydrogels with three different molar ratios of 1:1, 2:3, and 3:2 were investigated. The hydrogel with the 1:1 ratio has zeta potentials of −8.15, −17.1, and −37 mV at pH values of 3, 7, and 11 respectively, proving that the hydrogel membrane is negatively charged [29]. Specially, the surface of the hydrogel membrane is negatively charged in the neutral condition, showing cation selective.

In order to evaluate the wettability of the as-prepared AM/SPAK hydrogels, the water contact angle was measured. As shown in Fig. S3 (Supporting information), the contact angle is 84.9°, and hydrophilicity greatly enhances the water flux and ion transport in the membrane [30]. Moreover, the surface of the membrane is negatively charged, so the hydrogel can attract cations and repel anions, which is conducive to improving the osmotic energy conversion performance [31].

Fig. 2f shows the schematic of ion transport and osmotic energy harvesting process, and a homemade setup was used to test osmotic energy harvesting performance of the hydrogel membranes (Fig. S4 in Supporting information). In order to further explore the ion transport and osmotic energy conversion of the hydrogel membranes, the effect of potassium chloride (KCl) on the *I-V* curves at different concentrations was investigated. A series of hydrogel membranes with different proportions of AM/SPAK (1:1, 2:3, and 3:2, respectively) were prepared, with the thickness of 500 μm. As shown in Fig. S5 (Supporting information), the *I-V* curves of the hydrogel membranes are all linear and show linear ohmic behavior, indicating that the hydrogels have homogeneous symmetrical structure [14,32,33].

Then, the *I-V* curves data was used to calculate the conductivity (Notes S1 and S2 in Supporting information). As the concentration of the solution increases, the conductivity of the hydrogel membranes also has a linear correlation with the concentration (Fig. S6 in Supporting information). However, at low solution concentration, the transmembrane conductance of ions deviates significantly from the bulk value, and the lower the concentration, the more obvious the deviation is, indicating that the ion migration is controlled by the surface charge [34].

In the electrolytic cell, the KCl concentration in the low concentration side was 10^{-5} mol/L, and the other side was set from 10^{0} mol/L to 10^{-4} mol/L to perform gradient transformation. The short circuit current (I_{sc}) and open circuit voltage (V_{oc}) of AM/SPAK hydrogel membranes were measured. V_{oc} of the AM/SPAK hydrogel membrane increases from 52.32 mV to 356.7 mV with increasing concentration gradient, and I_{sc} increases from 0.048 μA to 0.297 μA (Fig. 2g).

The composite hydrogels show the cation selectivity (t_n) of 0.92, 0.91, 0.9, 0.88, and 0.85 from 10-fold to 100,000-fold KCl concentration gradients (Fig. 3a), corresponding to energy conversion efficiency (η) of 35.28%, 33.62%, 32%, 28.88%, and 24.5%, respectively (Fig. 3b and Table S1 in Supporting information). It can be found that the concentration has little influence on ion selectivity, which is because that AM/SPAK hydrogel has many negative charges and the distribution of pores [35,36]. However, the change of energy conversion efficiency is relatively large, and the reason is that as the electrolyte concentration increased, the thinner the electrical double layers, the weaker the ability to control ion transport [37-39]. The high cation selectivity and power density of AM/SPAK hydrogel membranes demonstrate their potential for high performance osmotic energy generation applications.

As shown in Figs. 3c and d, when the ratio of AM/SPAK is 1:1, and the thickness of the hydrogel membranes is 500 μm, the power and current densities for AM/SPAK hydrogel membranes were evaluated at three salinity gradients of 5- (0.05/0.01 mol/L

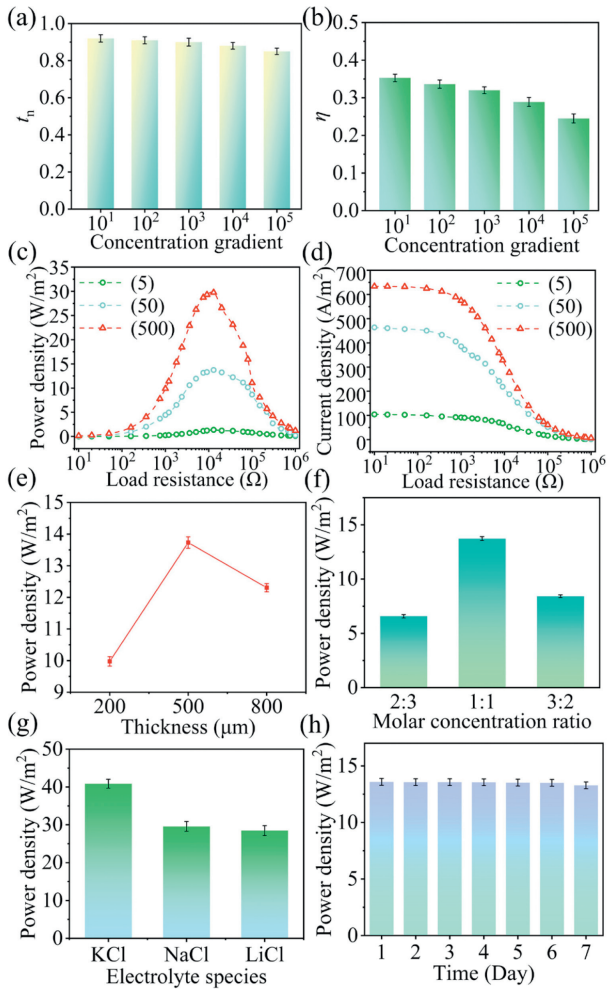

Fig. 3. Ion transport properties of the AM/SPAK hydrogel membrane. (a) Ion selectivity of the AM/SPAK hydrogel under five concentration gradients. (b) Energy conversion efficiency of the AM/SPAK hydrogel under five concentration gradients. (c) Power and (d) current densities of the AM/SPAK hydrogel under three salinity gradients. (e) The maximum power density of the AM/SPAK hydrogel membranes with different thicknesses at a 50-fold salinity gradient. (f) Power density with different AM/SPAK ratio for the thickness of 500 μm. (g) The maximum power density of the AM/SPAK hydrogel membranes with different electrolytes. (h) Stability of the AM/SPAK hydrogel in 7 days.

NaCl), 50- (0.5/0.01 mol/L NaCl), and 500-fold (5/0.01 mol/L NaCl), respectively. Compare with 2:3 and 3:2 (Fig. S7 in Supporting information), the power densities can reach 1.37 W/m^2 (5-fold), 13.73 W/m^2 (50-fold), and 29.73 W/m^2 (500-fold), and the current densities are 104.35 A/m^2 (5-fold), 463.88 A/m^2 (50-fold), and 633.44 A/m^2 (500-fold) respectively, showing the possibility of collecting osmotic energy in brackish water (5-fold), seawater (50-fold) and salt lake (500-fold) during mixing with rivers [40].

In addition, the effect of thickness of the hydrogel on the power density was also studied. The power densities of the AM/SPAK hydrogel membranes with three thicknesses (200, 500, and 800 μm) were investigated. As shown in Fig. 3e and Fig. S8 (Supporting information), the maximum power density of the hydrogel membrane is the highest when the thickness is 500 μm. For the thin hydrogel membrane, the functional groups are less sufficient to achieve the optimal power density. However, the spatial potential resistance increases and the transmembrane ion flux decreases for the thicker hydrogel membrane, resulting in a decrease in power density [31,41]. Fig. 3f shows that 1:1 of AM to SPAK performs the highest power density with thickness of 500 μm. As shown in

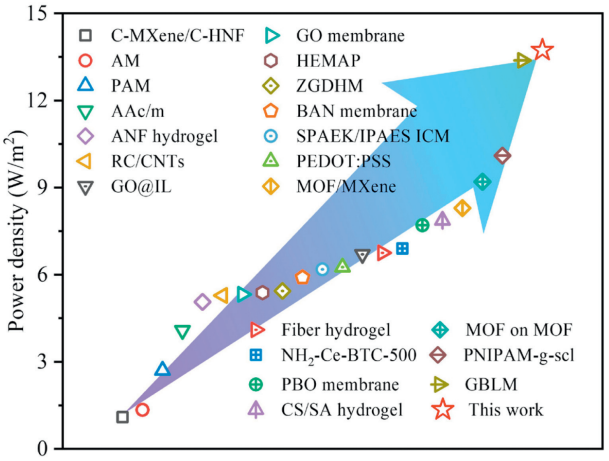

Fig. 4. Comparison of the power density with previous work at a 50-fold concentration gradient.

Fig. 3g, the maximum output power densities of the AM/SPAK hydrogel membrane (500 μm) in KCl, NaCl, and LiCl solutions were 40.86 ± 1.16, 29.57 ± 1.28, and 28.48 ± 1.32 W/m^2 respectively, following the general trend of KCl > NaCl > LiCl. The efficiency of charge separation is proportional to the diffusion rate with cations, and since the diffusion coefficient of K^+ is the largest (1.96×10^{-9} m^2/s), resulting in the maximum power density. While the diffusion coefficient of Li^+ is the smallest (1.03×10^{-9} m^2/s), so the smallest power density is obtained [42,43].

The long-term working stability of the AM/SPAK composite hydrogel membrane for osmotic energy conversion was also investigated. As shown in Fig. 3h, the composite hydrogel still maintains the power output after 7 days, and the power density is higher than 12.48 W/m^2 under a 50-fold salinity gradient, only decayed by 9.1%. The prepared AM/SPAK hydrogel performed good long-term working stability, indicating great application viability for harvesting osmotic energy.

The performance of AM hydrogels has also been characterized, and the results reveal that the AM/SPAK composite hydrogel membrane exhibits superior performance (Figs. S9 and S10 in Supporting information). Moreover, the power density obtained in this study was also compared with previously reported membranes (Fig. 4), and the details are shown in Table S2 (Supporting information). Comparing with other state-of-art membranes reported in recent years, the power density of our designed membrane is higher than most of them, showing great potential for efficient osmotic energy conversion.

In this work, the AM/SPAK hydrogel was successfully synthesized utilizing APS as a thermal initiator, TEMED serving as a catalyst, and BIS as the crosslinker. The successful cross-linking of AM and SPAK was confirmed through FTIR and XPS analysis. Furthermore, SEM and EDS results revealed that the hydrogel exhibited a porous and homogeneous structure. By optimizing the monomer concentration ratio and thickness screening, the optimal performance was determined when the ratio of AM/SPAK was 1:1 and the thickness was 500 μm. Due to the hydrogel's spatial negative charge and its distinct ion transport network structure, the AM/SPAK composite membrane exhibited superior cation selectivity. In simulated seawater/river water with a 50-fold NaCl concentration gradient (0.5 mol/L/0.01 mol/L), it achieved a maximum output power density of 13.73 W/m^2, outperforming the commercial benchmark of 5 W/m^2. Therefore, the AM/SPAK hydrogel represents an exceptional material for enhancing ion transport through membranes, and elevating osmotic energy harvesting. Its implementation in high-performance osmotic energy generator systems holds

immense potential and offers innovative insights for integrated energy designs.

Declaration of competing interest

The authors declare that they have no known competing financial interests or personal relationships that could have appeared to influence the work reported in this paper.

CRediT authorship contribution statement

Guilong Li: Writing – original draft, Visualization, Software, Methodology, Investigation, Formal analysis, Data curation. **Wenbo Ma:** Writing – original draft, Methodology, Investigation, Data curation. **Jialing Zhou:** Visualization, Validation. **Caiqin Wu:** Writing – review & editing, Formal analysis. **Chenling Yao:** Visualization, Software. **Huan Zeng:** Writing – review & editing. **Jian Wang:** Writing – review & editing, Supervision, Resources, Project administration, Funding acquisition, Conceptualization.

Acknowledgment

The authors would like to acknowledge the financial support by the National Natural Science Foundation of China (No. 21805017).

Supplementary materials

Supplementary material associated with this article can be found, in the online version, at doi:10.1016/j.cclet.2024.110449.

References

[1] S. Chu, A. Majumdar, Nature 488 (2012) 294–303.
[2] B.E. Logan, M. Elimelech, Nature 488 (2012) 313–319.
[3] Q. Luo, P. Liu, L. Fu, et al., ACS Appl. Mater. Interfaces 14 (2022) 13223–13230.
[4] S. Chae, H. Kim, J.G. Hong, et al., Chem. Eng. J. 452 (2023) 139482.
[5] G. Bian, N. Pan, Z. Luan, et al., Angew. Chem. Int. Ed. 60 (2021) 20294–20300.
[6] L. Ding, D. Xiao, Z. Zhao, et al., Adv. Sci. 9 (2022) 2202869.
[7] C. Li, H. Jiang, P. Liu, et al., J. Am. Chem. Soc. 144 (2022) 9472–9478.
[8] T. Xiao, J. Ma, Z. Liu, et al., J. Mater. Chem. A 8 (2020) 11275–11281.
[9] Y. Zhang, H. Wang, J. Wang, et al., Chem. Asian J. 18 (2023) e202300876.
[10] Y.H. Hu, Y.F. Teng, Y. Sun, et al., Nano Energy 97 (2022) 107170.
[11] J.W. Post, J. Veerman, H.V.M. Hamelers, et al., J. Membr. Sci. 288 (2007) 218–230.
[12] Z. Zhang, L.P. Wen, L. Jiang, Nat. Rev. Mater. 6 (2021) 622–639.
[13] Y. Zou, P.C. Tan, B.J. Shi, et al., Nat. Commun. 10 (2019) 2695.
[14] J. Wang, Y. Zhou, L. Jiang, Acc. Mater. Res. 4 (2023) 86–100.
[15] L. Yu, M. Wang, X. Li, et al., Chin. Chem. Lett. 34 (2023) 107785.
[16] W.W. Xin, L. Jiang, L.P. Wen, Acc. Chem. Res. 54 (2021) 4154–4165.
[17] X. Tong, S. Liu, J. Crittenden, et al., ACS Nano 15 (2021) 5838–5860.
[18] W.P. Chen, Q. Wang, J.J. Chen, et al., Nano Lett. 20 (2020) 5705–5713.
[19] B. Bao, J.R. Hao, X.J. Bian, et al., Adv. Mater. 29 (2017) 1702926.
[20] Y. Jiang, Y.X. Chen, W.Q. Feng, et al., Chem. Eng. J. 484 (2024) 149460.
[21] F.A. Dorkoosh, J. Brussee, J.C. Verhoef, et al., Polymer 41 (2000) 8213–8220.
[22] T. Mai, K. Wolski, A. Puciul-Malinowska, et al., Polymers 10 (2018) 1165.
[23] T. Ma, E. Balanzat, J.M. Janot, et al., ACS Appl. Mater. Interfaces 11 (2019) 12578–12585.
[24] G. Sennakesavan, M. Mostakhdemin, L.K. Dkhar, A. Seyfoddin, S.J. Fatihhi, Polym. Degrad. Stab. 180 (2020) 109308.
[25] H.V. Chavda, C.N. Patel, Int. J. Pharm. Investig. 1 (2011) 17–21.
[26] K. Chen, Y.M. Yang, H. Zhao, et al., Environ. Sci. Pollut. Res. 30 (2023) 46900–46912.
[27] K. Kabiri, A. Azizi, M.J. Zohuriaan-Mehr, et al., J. Appl. Polym. Sci. 120 (2011) 3350–3356.
[28] F. Sheng, B. Wu, X. Li, et al., Adv. Mater. 33 (2021) 2104404.
[29] M.C. Zhang, K.C. Guan, Y.F. Ji, et al., Nat. Commun. 10 (2019) 1253.
[30] Z.X. Gao, Z. Sun, M. Ahmad, et al., Carbohydr. Polym. 280 (2022) 119023.
[31] Z. Zhang, L. He, C. Zhu, et al., Nat. Commun. 11 (2020) 875.
[32] M.Y. Chen, K. Yang, J. Wang, et al., Adv. Funct. Mater. 33 (2023) 2302427.
[33] C. Zhu, L. Xu, Y. Liu, et al., Nat. Commun. 15 (2024) 4213.
[34] C.Y. Lin, T.J. Ma, Z.S. Siwy, et al., J. Phys. Chem. Lett. 11 (2020) 60–66.
[35] C. Sheng, Y. Tang, Y. Yao, et al., ACS Appl. Polym. Mater. 6 (2024) 4556–4567.
[36] S. Wang, Y. Zhang, Y. Han, et al., Acc. Mater. Res. 2 (2021) 407–419.
[37] L. Paoli, J. Cullen, Energy 192 (2020) 116228.
[38] Y. Zhou, X. Liao, J. Han, et al., Chin. Chem. Lett. 31 (2020) 2414–2422.
[39] M. Tsutsui, W.L. Hsu, K. Yokota, et al., Exploration 4 (2024) 20220110.
[40] X.B. Zhu, J.R. Hao, B. Bao, et al., Sci. Adv. 4 (2018) eaau1665.
[41] Y. Chen, Z. Zhu, Y. Tian, et al., Exploration 1 (2021) 20210101.
[42] S. Bae, D. Kim, H. Kim, et al., Adv. Funct. Mater. 30 (2020) 1908492.
[43] C. Wang, F.F. Liu, Z. Tan, et al., Adv. Funct. Mater. 30 (2019) 1908804.